

# Contributions of Dysregulated Energy Metabolism to Type 2 Diabetes Development in Nzo/H1Lt Mice With Polygenic Obesity

Robert A. Koza, Kevin Flurkey, Dawn M. Graunke, Christopher Braun, Huei-Ju Pan, Peter C. Reifsnnyder, Leslie P. Kozak, and Edward H. Leiter

**New Zealand Obese (NZO) male mice develop a polygenic juvenile-onset obesity and maturity-onset hyperinsulinemia and hyperglycemia (diabetes). Here we report on metabolic and molecular changes associated with the antidiabetes action of CL316,243 (CL), a  $\beta_3$ -adrenergic receptor agonist. Dietary CL treatment initiated at weaning reduced the peripubertal rise in body weight and adiposity while promoting growth without suppressing hyperphagia. The changes in adiposity, in turn, suppressed development of hyperinsulinemia, hyperleptinemia, hyperlipidemia, and hyperglycemia. These CL-induced alterations were reflected by decreased adipose tissue mass, increased expression of transcripts for uncoupling protein-1 (UCP-1), peroxisome proliferator-activated receptor alpha (PPAR $\alpha$ ), peroxisome proliferator-activated receptor coactivator-1 (PGC-1), and robust development of brown adipocyte function in white fat. Increased drug-mediated energy dissipation elicited a 1.5°C increase in whole body temperature under conditions of increased food intake but with no change in physical activity. Indirect calorimetry of mice treated with CL showed both increased energy expenditure and a restoration of a prominent diurnal pattern in the respiratory exchange ratio suggesting improved nutrient sensing. Our data suggest that CL promotes increased energy dissipation in white and brown fat depots by augmenting thermogenesis and by metabolic re-partitioning of energy in a diabetes-protective fashion. This is the first report demonstrating the effects of dietary  $\beta_3$ -agonist in preventing the onset of diabetes in a polygenic rodent model of type 2 diabetes.**

© 2004 Elsevier Inc. All rights reserved.

**T**HE MAJORITY of obesity-associated forms of type 2 diabetes (T2D) in humans is polygenic rather than monogenic in origin.<sup>1,2</sup> The animal models used to study this complex disease primarily have been those with severe monogenic obesity produced by defects in the leptin gene *Lep<sup>ob</sup>* mice or in its receptor (*Lep<sup>rd</sup>* mice and Zucker fatty *Lep<sup>fa</sup>* rats). While these studies have provided valuable insight on novel metabolic pathways related to obesity and the onset of hyperglycemia, a complex trait, such as T2D, is most accurately represented by polygenic models that do not exhibit loss-of-function mutations in the leptin-leptin receptor axis.<sup>3</sup> New Zealand Obese (NZO) mice of both sexes were specifically selected for juvenile-onset, polygenic obesity. Not surprisingly, genetic analyses have shown a large number of quantitative trait loci (QTL) controlling body mass and/or adiposity in the genome of this strain.<sup>4-6</sup> Although both the leptin and leptin receptor genes in NZO mice appear to function normally,<sup>7</sup> peripheral but not central resistance to leptin develops.<sup>8</sup> A defect in leptin transport across the blood-brain barrier has been reported.<sup>9</sup> Hepatic and skeletal muscle insulin resistance and elevated hepatic glucose production are present by 4 to 6 weeks of age.<sup>10</sup> Indeed, the obesity itself has been proposed as a primary cause of the increased hepatic glucose output and the associated altered carbohydrate metabolism because these characteristics are mimicked in New Zealand Chocolate (NZC) mice fed a high-fat diet.<sup>11</sup>

Whereas NZO mice of both sexes develop juvenile-onset obesity, obesity-induced diabetes (diabetes) is limited to males and operates as a threshold event requiring interaction among multiple genes as well as environmental components.<sup>4,5</sup> Currently, NZO/H1Lt exhibit spontaneous diabetic frequencies between 40% and 60% by 20 weeks of age. The rate of weight gained during the maturational period (4 to 8 weeks after birth) represents an important risk factor determining which males transit from impaired glucose tolerance (IGT) to chronic non-fasting hyperglycemia.<sup>4,5,12</sup> Hence, NZO/H1Lt male mice are particularly useful for the study of the physiologic and endo-

crinologic changes required for an obesity syndrome to shift from IGT to a complete loss of glucose homeostasis.

In the present report, CL316,243 (CL), a  $\beta_3$ -adrenergic receptor agonist with potent anti-obesity activity in a variety of obese mice,<sup>13</sup> was used to explore the effects and mechanisms of  $\beta_3$ -agonist stimulation on obesity-induced diabetes in NZO/H1Lt males. The anti-obesity effect of such agonists in rodents is possibly mediated through stimulation of brown adipose tissue (BAT) thermogenesis.<sup>14</sup> Poor reproductive performance, often seen in obese rodents, was improved in NZO/H1Lt mice by a 1-month exposure to CL fed at 0.001% (wt/wt) in the diet. This 1-month period of CL-supplemented diet prevented the rapid, early development of adiposity and subsequently normalized the hypothalamic-pituitary-gonadal axis such that reproductive performance was markedly enhanced (unpublished observations). This finding suggests that chronic CL feeding might be used to modulate defects in energy utilization that trigger diabetes development during maturation in NZO/H1Lt males. Therefore, we undertook a longitudinal analysis of endocrine and metabolic factors associated with the onset of diabetes in NZO/H1Lt males, and characterized alterations in gene expression and metabolic patterns associated with  $\beta_3$ -

---

From the Pennington Biomedical Research Center, Baton Rouge, LA; The Jackson Laboratory, Bar Harbor, ME; and Thermogenic Imaging Inc, North Billerica, MA.

Submitted September 30, 2003; accepted December 12, 2003.

Supported by National Institutes of Health Grants No. DK56853 (E.H.L.) and DK58152 (L.P.K.). Institutional shared services at The Jackson Laboratory were supported by National Cancer Institute Cancer Center Support Grant No. CA34196.

Address reprint requests to Robert A. Koza, PhD, The Pennington Biomedical Research Center, 6400 Perkins Rd, Baton Rouge, LA 70808-4124.

© 2004 Elsevier Inc. All rights reserved.

0026-0495/04/5306-0007\$30.00/0

doi:10.1016/j.metabol.2003.12.024

agonist-mediated prevention of diabesity in a polygenic animal model.

## MATERIALS AND METHODS

### *Animals and Treatment*

NZO/HILt mice are a substrain of NZO/HI mice formerly maintained by Dr L. Herberg at the Diabetes Research Institute, Düsseldorf, Germany. The NZO/HILt substrain at The Jackson Laboratory was derived from in vitro fertilization using gametes from a single brother/sister pair. A/J males obtained from The Jackson Laboratory's animal resources unit were used for some comparisons. Mice were maintained under conventional specific pathogen-free conditions in a room with controlled temperature and humidity and a 12/12-hour light/dark cycle. Male mice used for analysis were housed 2 to 4 per pen and given ad libitum access to water and food. Control males received a nonsupplemented National Institutes of Health (NIH)-31 diet containing 4% fat (Purina, Richmond, IN). CL-treated males were treated with the  $\beta_2$ -adrenergic agonist custom-prepared by the manufacturer in the pelleted NIH-31 diet (0.001% [wt/wt] CL, kindly provided by Dr K. Steiner, Wyeth-Ayers, Princeton, NJ). Weanling mice were placed on control or CL-containing diet at 4 weeks of age and maintained on these diets for 18 weeks.

### *Physiologic and Endocrinologic Monitoring*

Body weights were monitored weekly throughout the study. Food intake was monitored by measuring food consumption daily at 8- and 20-week time points (daily measurements over a 7-day period); unconsumed food in the bottom of the cages was sieved away from bedding material and feces and the weight subtracted from the weight of food removed from the food compartment. Nonfasting glucose, insulin, and leptin concentrations in plasma were determined as described previously at the intervals noted in the figures.<sup>3</sup> Mice were killed at 8 or 22 weeks of age, with tissues collected, weighed, and either snap-frozen in liquid nitrogen or immediately homogenized in TriReagent (Molecular Research Center, Cincinnati, OH) or Trizol (GIBCO-BRL, Rockville, MD) for RNA isolation. Sections of pancreas, liver, and inguinal fat from each mouse were also fixed in Bouin's solution for histopathological analysis. Pancreases were stained with aldehyde fuchsin to detect granulated islet beta cells. Liver was stained with periodic acid-Schiff (PAS) reagent to detect glycogen. Fat tissue was stained with hematoxylin and eosin. In some mice, individual fat pads were dissected and weighed to establish changes in specific fat depots. Dual-emission x-ray absorptiometry (DEXA) was used to assess changes in lean versus fat body composition as described previously<sup>3</sup> using a bone densitometer (Piximus, LUNAR Instruments, Madison, WI). The instrument calculates percent fat using the formula (total fat/body weight)  $\times$  100, with the head excluded from the analysis. At necropsy, serum obtained by heart puncture was assayed for cholesterol, triglycerides, and blood urea nitrogen (BUN) with a clinical chemistry analyzer (Synchron 5, Beckman Instruments, Fullerton, CA).

### *Gene Expression Analysis*

RNA for real-time quantitative reverse-transcriptase polymerase chain reaction (QRT-PCR) was isolated using TriReagent or Trizol as described by the manufacturers. QRT-PCR using SYBR Green (Applied Biosystems, Foster City, CA) was performed for genes in Table 3 as detailed elsewhere.<sup>15</sup> Methods and all gene-specific primer sequences generated using Primer Express can be found at: [www.jax.org/staff/leiter/labsite/databases.html](http://www.jax.org/staff/leiter/labsite/databases.html). Non-multiplexed reactions with gene-specific TaqMan (Applied Biosystems, Foster City, CA) probes and primer sets were used to measure the expression of uncoupling protein-1 (UCP-1), peroxisome proliferator-activated receptor alpha (PPAR $\alpha$ ), and peroxisome proliferator-activated receptor coactivator

1 $\alpha$  (PGC-1 $\alpha$ ) mRNAs as described elsewhere.<sup>16</sup> Cyclophilin mRNA was used to control for RNA variability in a separate reaction with the diluted RNA sample. Standard curves were generated for each QRT-PCR run using brown fat RNA as previously described.<sup>16</sup> Real-time fluorescence detection was performed using either an ABI 7700 Sequence Detector or an ABI 7900HT Sequence Detection System (Applied Biosystems).

### *Thermal Signature Analysis Imaging*

The Thermal Signature analysis (TSA) ImagIR system (Thermogenic Imaging, North Billerica, MA) is a novel technology that employs real-time, highly sensitive quantification of infrared thermographic images to detect tissue specific thermogenesis (3- to 5- $\mu$ m wavelength) in animal models. All mice were shaved 24 hours prior to imaging using animal hair clippers on their dorsal surfaces to expose the skin covering the interscapular BAT depot. Mice received anesthesia induction for 3 minutes using 5% isoflurane in oxygen. Mice were rapidly removed from the anesthesia induction chamber to the ImagIR imaging chamber platen and placed in individual pens with anesthesia delivery nose ports. A light anesthetic plane was maintained while mice were inside the imaging chamber by administering 2.5% isoflurane in oxygen at a flow rate of 0.125 L/min/animal. The surface temperature of the platten was automatically maintained at  $37 \pm 0.1^\circ\text{C}$ . Groups of 8 control and treated animals were imaged simultaneously for 20 minutes. Thermographic images were taken once per minute using a 2-dimensional  $256 \times 256$  pixel PtSe sensor array (Thermogenic Imaging). The images taken at each 1-minute interval were obtained by averaging 16 consecutive image frames being continuously recorded at a rate of 60 Hz. Following imaging, the imaging chamber was evacuated of isoflurane and animals were removed and recovered.

TSA infrared images were analyzed using Heat SeekIR software version 1.03 (Thermogenic Imaging). Each infrared image of all 8 animals positioned in the imaging chamber had a resolution of  $256 \times 256$  pixels with each pixel having a temperature value proportional to the amount of infrared radiation being detected by the sensor. Images were artificially colorized to produce contrast and regions of interest (ROI) were drawn over the area corresponding to the location of the BAT. ROIs were copied to all 8 animals in a given assay and the mean temperature of all pixels within a given ROI was reported as being the value for a given animal at a given time point. Each BAT ROI value for each animal in a given image was corrected for thermal sensor drift and variation by using an internal absolute temperature reference. ROIs were also drawn to measure the whole back temperature of each animal.

### *Metabolic Cages and Indirect Calorimetry*

Eight-week-old NZO males maintained from weaning on control diet (NIH-31, 4% fat) were fed with this diet for an ensuing 2-week period, or switched to CL-supplemented diet for 2 weeks before being placed into Comprehensive Lab Animal Monitoring System (CLAMS; Columbus Instruments, Columbus, OH) metabolic cages. These consist of individual live-in cages instrumented for automated, noninvasive data collection. Each cage is an indirect open circuit calorimeter to provide measures of oxygen consumption and carbon dioxide production, thus automatically calculating the respiratory exchange ratio (RER;  $\text{VCO}_2/\text{VO}_2$ ) and heat production (kilocalories per day) at hourly intervals. The cages also provide concurrent measurements of ingestive behavior and activity. Physical activity (total movement, ambulatory activity, and rearing behavior) is continuously measured by a dual array of infrared beams surrounding each cage. Data collection commenced as soon as all animals were in the cages and continued for 3 consecutive 24-hour periods. Automated collection of food consumption data was not possible because the mice were too large to access food via a "reach-in" tube connecting to a food hopper over the gravimetrically monitored system. Accordingly, the tube was blocked using a paper clip (still

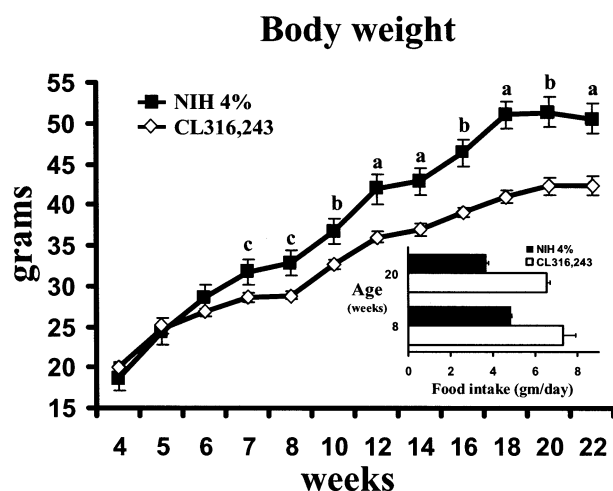


**Fig 1.** CL316,243-mediated changes in body weight and food consumption. (A) CL-mediated retardation of body weight gain. Differences are significant at <sup>a</sup> $P \leq .001$ , <sup>b</sup> $P \leq .001$ , and <sup>c</sup> $P \leq .05$  by 2-way ANOVA ( $n = 5$  control and 8 CL-treated mice per group). (B) CL-mediated increase in food consumption. Food consumption was measured at 8 and 20 weeks for a period of 1 week using 6 mice per group as described in the methods.

allowing airflow) and pelleted food was spread on the cage floor (an elevated grid allowing urine and feces to be absorbed by blotting paper). RER and energy expenditure (EE; heat) data were calculated and presented for each of the 3 days, as well as for the light and dark cycles. Average daily, light and dark cycle values were also calculated for the 3-day period.

#### Statistical Analysis

Data analysis was performed using Microsoft Excel and StatView (version 4.5; Abacus Concepts, San Francisco, CA). All values reported are the mean  $\pm$  SEM for each group. Statistical significance between groups was calculated by analysis of variance (ANOVA) or by unpaired  $t$  test. Differences were considered to be significant if  $P \leq .05$ .

### RESULTS

#### Effect of CL316,243 on Development of Diabetes

Data in Fig 1 show that CL feeding retarded the early increase in body weight that typified the rapid development of juvenile obesity in control diet-fed NZO/HILt males. This retardation in rate of weight gain was evident by the second week of treatment. CL-fed males typically gained 20% to 50% less weight than controls each week until the mice were 18 weeks old, at which point some control NZO/HILt males stopped gaining weight. This demonstrates that desensitization to CL developed slowly, if at all, over a 3-month period. This observation is consistent with previously published reports showing lack of tachyphylaxis in some inbred mouse strains after long-term exposure to CL.<sup>17</sup> Interestingly, this retardation in weight gain was not correlated with a reduction in hyperphagia; on the contrary, CL-fed males consumed significantly ( $\sim 40\%$ ) more food than control diet-fed males at both the 8- and 20-week time points (Fig 1; inset). Plasma triglycerides ( $166 \pm 7$  v  $35 \pm 4$  mg/dL;  $P < .0001$ ;  $n = 6$  per group) and cholesterol ( $156 \pm 7$  v  $109 \pm 5$  mg/dL;  $P < .001$ ;  $n = 6$  per

group) were significantly lower in 8-week-old mice after dietary CL treatment compared with control animals, whereas BUN was more than 30% higher in the same CL-treated animals ( $19.3 \pm 0.7$  v  $30 \pm 0.9$  mg/dL;  $P < .0001$ ;  $n = 6$  per group). The observed increase in plasma BUN levels in CL-fed mice may be the result of the elevated protein and amino acid catabolism needed to compensate for the higher energy requirement in these animals.

Evidence that CL was augmenting energy utilization in NZO/HILt mice was indicated by DEXA analysis (Table 1). Total fat mass in the CL-fed males was one third of the mass in controls, accounting for two thirds of the body weight difference between CL-fed and control males. Lean mass was 14% less in CL-fed males, coincident with a 16% lower bone mineral content. Because bone area was unaffected, the bone density was also lower in CL-fed males. Thus, the CL-mediated decrease in whole body mass entailed reductions in bone density as well as in lean and fat mass.

Data in Fig 2 demonstrate the potent antidiabetic effect of CL treatment. Although the hyperphagia and the rapid rate of pre-maturational weight gain do not distinguish the polygenic NZO/HILt diabetes model from most monogenic obesity/diabetes models, the polygenic model is sharply different from the others in terms of the maturity-onset development of insulin and leptin resistance, as well as overt hyperglycemia development after 12 weeks and well after puberty. At 12 weeks of age, glycemic values of control and CL-treated males fell within a normal range, as did plasma levels of insulin and leptin. Plasma insulin levels increased progressively in the control group such that by 22 weeks, 6 of 12 NZO/HILt mice were clearly diabetic (glucose  $> 300$  mg/dL) and 4 of the remaining 6 had plasma glucose ranging between 200 and 300 mg/dL. CL-mediated reduction in insulinogenic stress on the pancreatic beta cells was confirmed by pancreatic histopathology (Fig 3A and B). Atrophic islets comprised of partially to completely degranulated beta cells in pancreata of 22-week-old hyperglycemic control males (Fig 3A) contrasted sharply with the well-granulated beta cells in hyperplastic islets from the age-matched, normoglycemic CL-treated males (Fig 3B).

#### Cellular and Molecular Effects of CL316,243 on Specific Fat Depots

Data in Table 2 show CL-mediated reduction in mass of all adipose tissue depots measured. All fat pad weights, but most notably retroperitoneal and epididymal fat, were significantly

**Table 1.** DEXA Analysis of 8-Week-Old Male NZO/HILt Mice After 4 Weeks on NIH-31 Chow Diet  $\pm$  CL316,243

	Control	CL316,243	P Value
Lean mass	28.2 $\pm$ 0.6	24.2 $\pm$ 0.8	.02
Fat mass	10.9 $\pm$ 0.5	3.6 $\pm$ 0.3	.0002
% Fat	27.9 $\pm$ 0.4	13.0 $\pm$ 0.8	<.0001
BMD	0.052 $\pm$ 0.0003	0.044 $\pm$ 0.001	.0009
BMC	0.397 $\pm$ 0.006	0.334 $\pm$ 0.016	.02
Bone area (cm <sup>3</sup> )	7.58 $\pm$ 0.12	7.51 $\pm$ 0.023	NS

NOTE. Data are mean  $\pm$  SEM ( $n = 3$  mice per group). Abbreviations: NS, nonsignificance by 2-way ANOVA; BMD, bone mineral density; BMC, bone mineral content.

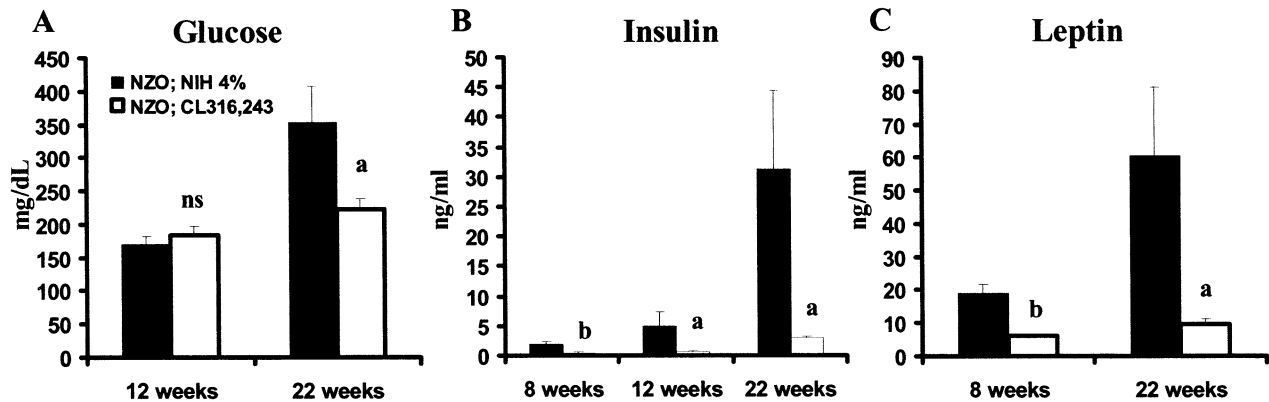


Fig 2. CL316,243-mediated suppression of diabetes development. (A) Plasma glucose measurement shows that chronic exposure to CL suppressed progression to hyperglycemia. (B) Plasma insulin measurement shows CL suppression of hyperinsulinemia. (C) Plasma leptin measurement shows CL suppression of hyperleptinemia. Glucose and insulin were measured in 5 control and 8 CL-fed NZO/HILt males. Leptin was analyzed in 13 control and 12 CL-fed mice at 8 weeks and 11 control and 8 CL-fed males at 22 weeks. Differences between control and CL-fed groups are significant at <sup>a</sup> $P \leq .05$  and <sup>b</sup> $P \leq .001$  (NS, not significant).

greater (3- to 6-fold) in control mice as compared with CL-fed mice at both 8 and 22 weeks. Although fat pad weights increased along with body weights between the 8- and 22-week time points in both control and CL-treated males, the percentage remained the same. The cumulative weight of BAT, inguinal, retroperitoneal fat, and epididymal fat averaged almost 3 g less in the CL-fed mice as compared to the control mice after 22 weeks and 2 g less after 8 weeks. Regardless of dietary regimen, the cumulative weights of the 4 fat pad weights measured in this study accounted for only 20% to 25% of the total fat content in the 8-week-old mice as determined by DEXA (Table 1). Comparative histology and PAS staining for glycogen in liver sections of 8-week-old mice revealed moderate levels of microvesicular lipidosis and reduced glycogen content in control compared to CL-fed animals (Fig 3C and D). Hepatic glycogen content in CL-fed mice appeared to be normal. Inguinal fat pads dissected from CL-fed males at 22 weeks were different in both size and coloration from those of controls. Besides being smaller and weighing less (Table 2), the inguinal fat pads of CL-fed mice were phenotypically brown in color, and somewhat resembled interscapular brown adipose tissue. Histological evaluation of inguinal fat pads from CL-fed mice revealed focal regions of multilocular cells resembling brown adipocytes, whereas the fat pads of control NZO mice contain mostly unilocular white adipocytes (Fig 3E and F).

#### Gene Expression Analysis

Analysis of the inguinal fat pads from 22-week-old CL-fed mice (Fig 4) confirmed BAT development by showing a greater than 50-fold increase in UCP-1 mRNA expression, a brown fat specific marker. Surprisingly, the levels of UCP-1 expression in the inguinal fat approached approximately 60% of that observed in interscapular brown fat of the control mice. UCP-1 expression was also elevated about 10-fold and 2.5-fold in retroperitoneal fat and interscapular brown fat, respectively, in the CL-fed mice. Interestingly, although no differences on PPAR $\gamma$  expression could be detected in the 3 fat pads (data not shown), both PPAR $\alpha$  and PGC-1 $\alpha$  mRNA levels were signif-

icantly increased in inguinal and retroperitoneal fat, and decreased in interscapular brown fat (Fig 4). PGC-1 $\alpha$  and PPAR $\alpha$  are considered to be important for regulating brown adipocyte differentiation and mitochondria biogenesis within adipocytes and muscle. Although it is not surprising to observe increased expression of these regulatory genes in white fat depots undergoing conversion to brown fat, it is interesting that PPAR $\alpha$  and PGC-1 $\alpha$  are downregulated in the BAT of mice after  $\beta_3$ -adrenergic stimulation. In data not shown,  $\beta_3$ -adrenergic receptor mRNA was also significantly elevated in the white fat depots (6- to 7-fold) but unchanged in BAT of CL-treated mice.

A survey of mRNA expression was performed in liver, muscle, and inguinal fat of 8-week old NZO males fed control or CL- supplemented diets. A list of all genes analyzed can be found at [www.jax.org/staff/leiter/labsite/databases.html](http://www.jax.org/staff/leiter/labsite/databases.html). Table 3 represents a summary of genes with significant differences of expression between control and CL-fed mice. Although most genes examined were not significantly different between control and CL-fed mice, both PPAR $\alpha$  (5.5-fold) and UCP-1 (6.1-fold) were significantly elevated in the CL-fed animals, corresponding to the data shown for the 22-week old mice (Fig 4). The increased levels of PPAR $\alpha$  and UCP-1 in inguinal WAT demonstrate the early changes in brown adipocyte development in this traditional WAT depot. Other genes exhibiting changes in RNA expression in inguinal fat include UCP-2 and hormone-sensitive lipase (HSL), which were decreased (3-fold) and increased (3-fold), respectively, by dietary CL.

Muscle exhibited increased HSL (5.1-fold) and myostatin (3.7-fold) and decreased UCP-3 (4.5-fold) mRNA levels as a result of dietary CL. The expression of adipisin, a subunit of the acylation-stimulating protein (ASP) complex, increased more than 10-fold in muscle, but decreased more than 14-fold in liver in response to dietary CL. Hepatic phosphatidylethanolamine N-methyltransferase (PEMT) expression was also shown to be elevated 3-fold in liver by dietary CL. PEMT catalyzes the conversion of phosphatidylethanolamine to phosphatidylcholine and is thought to be important for hepatic lipoprotein synthesis.<sup>18-20</sup>

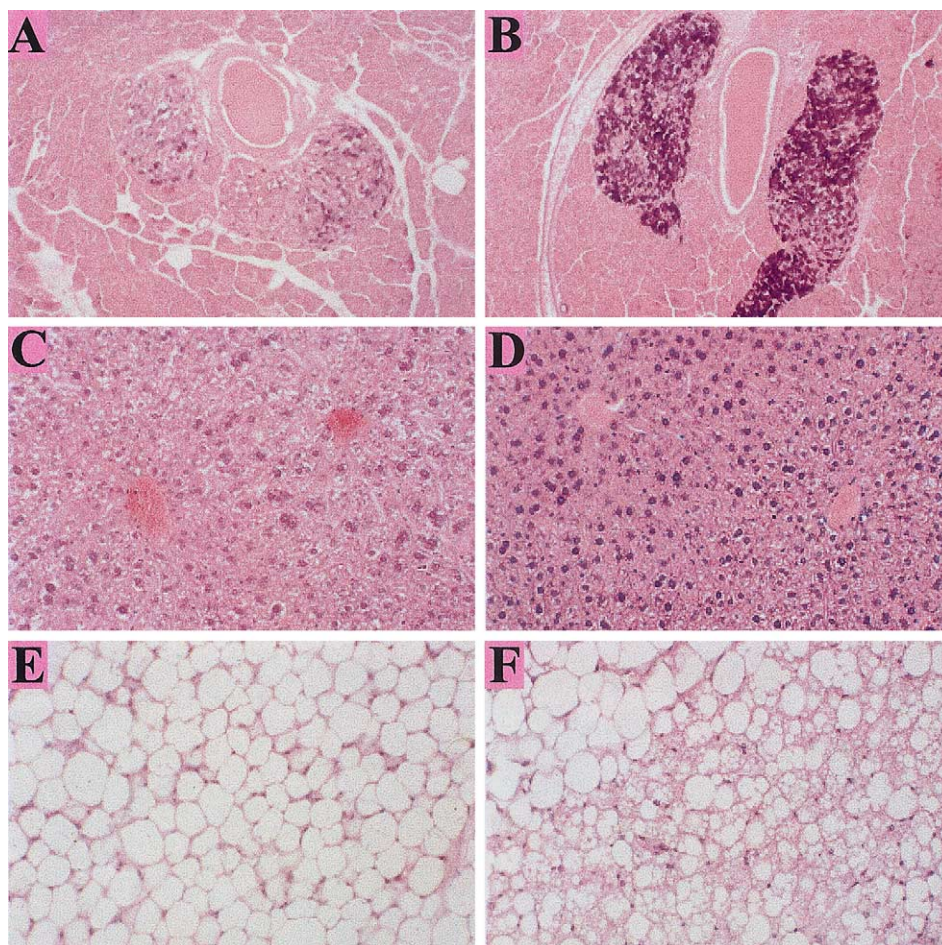


**Fig 3.** CL316,243-mediated preservation of pancreatic islet structure and beta-cell granularity and histologic changes in liver and inguinal fat. (A) Aldehyde fuchsin staining a diabetic 22-week-old NZO male fed control diet. Islets show atrophic changes and extensive beta-cell degranulation associated with hypersecretory activity (200x magnification). (B) Aldehyde fuchsin staining a normoglycemic 22-week-old NZO male fed CL-supplemented diet. Islets are enlarged and are constituted with heavily granulated beta cells denoting insulin storage rather than hypersecretion (200x magnification). (C) Periodic acid–Schiff staining of liver glycogen in a diabetic 22-week-old NZO/HILt male fed control diet. Moderate microvesicular lipidosis and reduced glycogen content are observed. (D) Liver of age-matched CL-treated (normoglycemic) 22-week-old male shows increased glycogen content and no lipidosis. (E) Hematoxylin and eosin staining of inguinal fat of a chow-fed, hyperglycemic (nondiabetic) NZO/Lt male at 22 weeks of age. Adipocytes show hypertrophy typical of NZO fat. (F) Hematoxylin and eosin staining of inguinal fat of a normoglycemic CL-treated, age-matched male shows both a striking reduction in the size of white adipocytes and the apparent emergence of brown adipocytes.

#### *Thermography and Indirect Calorimetry*

To examine whether increases of UCP-1 and brown adipocytes in white fat depots (ie, inguinal fat) contribute to increased heat production, TSA was used to measure the temperature of the interscapular and inguinal regions, as well as the entire back of the mouse (Fig 4). Data in the table in Fig 4 show significant CL-mediated temperature increases in all 3 areas in comparison with control animals. The most marked increases (1.57°C and 1.46°C) occurred in the inguinal and interscapular regions of the back, respectively. These data suggest that increased thermogenesis and heat output in dorsal and inguinal regions of CL-fed NZO/HILt mice occurs as a result of elevated UCP-1 activity and increased numbers of brown adipocytes.

RER and EE (heat) were measured by indirect calorimetry in an independent cohort of 8-week old NZO/HILt males fed

control diet or CL-supplemented diet for approximately 2 weeks. Data are summarized in Table 4. RERs were significantly elevated in CL-fed mice during both light and dark cycles compared to control animals. The magnitude in the difference between the light and dark cycles was much greater with the CL-fed mice ( $\Delta 0.084$ ), indicating a prominent diurnal cycle for RER, whereas very little difference in light/dark cycle variation of RER was observed with the control mice ( $\Delta 0.027$ ). The average nocturnal RER of the CL-fed mice (0.928; Table 4) is very close to the food quotient (FQ = 0.9296) calculated for the dietary composition used in this study. These data indicate a diurnal shift in energy utilization in the CL-fed animals that is not as apparent in the control mice. Cumulative daily EE, calculated as heat (kilocalories per day), was approximately 40% higher in CL-fed mice, especially during the dark



**Table 2. CL316,243-Mediated Changes in Body Weight and Fat Composition of NZO/HILt Mice**

Animal/Tissue Weights and Blood Chemistry	8 Weeks		22 Weeks	
	Control	+CL316,243	Control	+CL316,243
BW-initial; 4 wk (g)	23.65 ± 0.56	23.35 ± 0.57	18.70 ± 1.64	20.03 ± 0.51
BW-final; 8 or 22 wk (g)	41.68 ± 0.71	28.65 ± 1.03*	53.48 ± 1.95	42.39 ± 1.13†
BAT (g)	0.27 ± 0.01	0.15 ± 0.01*	0.42 ± 0.02	0.22 ± 0.02*
RP fat (g)	0.43 ± 0.02	0.08 ± 0.01*	0.61 ± 0.03	0.17 ± 0.01*
EPID fat (g)	1.53 ± 0.08	0.38 ± 0.06*	2.46 ± 0.13	0.77 ± 0.08*
ING fat (g)	0.50 ± 0.03	0.21 ± 0.01*	0.95 ± 0.05	0.40 ± 0.02*
Total fat (g)	2.72 ± 0.10	0.86 ± 0.08*	4.45 ± 0.15	1.55 ± 0.10*

NOTE. NZO/HILt males fed control or CL316,243-supplemented diets starting at 4 weeks of age were killed at 8 and 22 weeks of age and body weights, total fat and specific fat depot weights were measured. Fat pads collected and weighed included brown adipose tissue (BAT), retroperitoneal fat (RP fat), epididymal fat (EPID fat), and inguinal fat (ING fat). Data represent mean ± SEM for 6 control and 6 CL-treated males at 8 weeks and a separate cohort of 12 control and 8 CL-treated males at 22-weeks.

Differences between control and CL-treated groups were significant by 2-way ANOVA at \* $P < .0001$  and † $P < .001$ .

cycle (15.94 v 11.16 kcal/h;  $P < .005$ ), compared to control mice (Table 4). No differences in the activity profiles for CL-fed and control mice were observed (data not shown) and both groups of mice exhibited clear diurnal activity patterns with significantly increased nocturnal activity.

## DISCUSSION

Many studies have previously demonstrated the efficacy of  $\beta_3$ -adrenergic receptor stimulation in the prevention of obesity and T2D in monogenic rodent obesity models by cold-exposure or by the use of specific  $\beta_3$ -adrenergic receptor agonists, ie, CL316,243 (CL) or BRL37,344, administered acutely or chronically via intraperitoneal or subcutaneous injection, mini-osmotic pumps, or gastric tubes or as a food supplement.<sup>14,21-24</sup> Even though NZO/HILt mice do not exhibit the severe thermoregulatory defects observed in *Lep<sup>ob</sup>* or *Lepr<sup>db</sup>* mutant mice, our data show the same striking therapeutic effects of CL in NZO/HILt males as has been shown in the monogenic obesity models as well as in diet-induced obesity.<sup>13</sup> Polygenic rodent

obesity models, although complex, are becoming the focus of significant investigation because polygenic inheritance more accurately reflects the genetic basis of the more common forms of T2D in humans.<sup>3</sup> The genetics, hematology, and pancreatic histopathology of the NZO/HILt substrain have been reported in detail previously.<sup>3,25,26</sup> The present report shows that hyperinsulinemia and hyperleptinemia are relatively late to develop in NZO/HILt males, and the onset of hyperglycemia occurs even later. However, because obesity manifests in an early juvenile phase in these mice, altered energy metabolism and prevention of early onset increases in adiposity by CL treatment during early somatic growth has provided a useful probe

**Table 3. CL316,243-Mediated Changes in Gene Expression in Liver, Muscle, and Inguinal Fat**

Gene Analyzed	Tissue		
	Liver	Muscle	Inguinal Fat
Adipsin	14.3 ↓	10.5 ↑	↔
PPAR $\alpha$	↔	↔	5.5 ↑
UCP-1	ND	↔	6.1 ↑
UCP-2	↔	↔	3.0 ↓
UCP-3	ND	4.5 ↓	↔
PEMT	3.0 ↑	↔	↔
HSL	↔	5.1 ↑	3.0 ↑
Myostatin	ND	3.7 ↑	↔

NOTE. Data represent a subset of gene transcripts exhibiting significant differences ( $P \leq .05$ ) between 8-week-old NZO/HILt males fed NIH-31 ± CL316,243 as measured by QRT-PCR. Genes not listed in the table and showing no significant differences in all 3 tissues examined were FABP4 (aP2), FAS, LPL, PPAR $\gamma$ 1, ACC, ACO, PGC-1 $\alpha$ , DIO2, FAT/CD36, and FATP. Gene transcripts with no significant differences in inguinal fat and muscle include GLUT4 and TNF $\alpha$  and in inguinal fat and liver, CPT1 $\alpha$ , PPAR $\gamma$ 2, and CYP4A1. Genes examined in individual tissues included SREBP2, DGAT1, and CYP3A in liver, leptin, resistin, NF $\kappa$ B, and ACRP30 in inguinal fat and CPT1 $\beta$  and SREBP1c in muscle. The data in the table represent the mean fold difference for 3 mice per group. Vertical arrows indicate direction of change in relation to CL316,243-treated mice and horizontal double arrow indicates that no significant difference in gene expression was detected. A list of all gene transcripts analyzed and corresponding primer sequenced can be found at [www.jax.org/staff/leiter/labsite/databases.html](http://www.jax.org/staff/leiter/labsite/databases.html).

Abbreviation: ND, not determined.

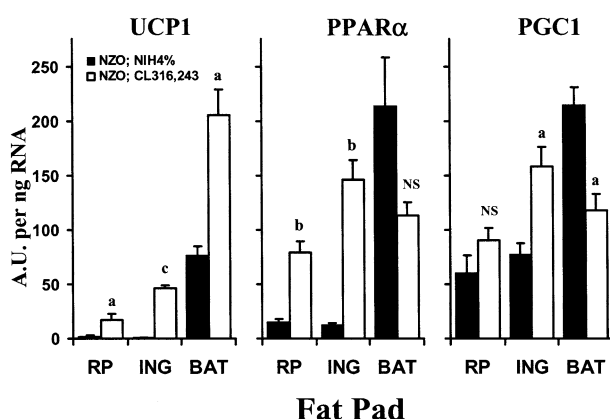


**Fig 4. CL316,243 induction of genes associated with brown fat thermogenesis in white fat of NZO mice.** UCP-1, PPAR $\alpha$ , and PGC-1 $\alpha$  mRNA expression was measured in retroperitoneal fat (RP), inguinal fat (ING), and interscapular brown fat (BAT) of age-matched 22-week-old control and CL-treated NZO/HILt ( $n = 3$ /group). Differences significant (ANOVA) at <sup>a</sup> $P < .05$ , <sup>b</sup> $P < .005$ , and <sup>c</sup> $P < .0005$  (NS, not significant).

**Table 4. CL316,243 Alterations in Energy Metabolism**

	RER ( $V_{CO_2}/V_{O_2}$ )		EE (kcal/d)	
	-CL316,243	+CL316,243	-CL316,243	+CL316,243
Day 1				
24 hours	0.762 $\pm$ 0.019	0.857 $\pm$ 0.037*	10.09 $\pm$ 1.06	13.59 $\pm$ 1.40†
Light	0.746 $\pm$ 0.036	0.811 $\pm$ 0.045 <sup>NS</sup>	8.56 $\pm$ 1.31	11.35 $\pm$ 1.20‡
Dark	0.776 $\pm$ 0.015	0.900 $\pm$ 0.038*	10.73 $\pm$ 1.46	14.61 $\pm$ 1.58†
Day 2				
24 hours	0.815 $\pm$ 0.017	0.899 $\pm$ 0.002†	10.19 $\pm$ 0.83	14.90 $\pm$ 2.17*
Light	0.794 $\pm$ 0.012	0.866 $\pm$ 0.035†	9.05 $\pm$ 0.63	13.00 $\pm$ 2.52‡
Dark	0.833 $\pm$ 0.024	0.928 $\pm$ 0.057‡	11.15 $\pm$ 1.23	16.51 $\pm$ 2.03*
Day 3				
24 hours	0.849 $\pm$ 0.025	0.913 $\pm$ 0.036‡	11.26 $\pm$ 0.98	15.67 $\pm$ 2.50†
Light	0.842 $\pm$ 0.025	0.864 $\pm$ 0.027 <sup>NS</sup>	10.18 $\pm$ 0.92	13.41 $\pm$ 2.55‡
Dark	0.855 $\pm$ 0.032	0.958 $\pm$ 0.048†	11.49 $\pm$ 1.00	16.81 $\pm$ 2.41*
Average (3 days)				
24 hours	0.808 $\pm$ 0.018	0.890 $\pm$ 0.033*	10.51 $\pm$ 0.50	14.72 $\pm$ 1.89*
Light	0.794 $\pm$ 0.023	0.846 $\pm$ 0.031‡	9.19 $\pm$ 0.49	12.52 $\pm$ 2.06‡
Dark	0.821 $\pm$ 0.016	0.928 $\pm$ 0.042*	11.16 $\pm$ 0.77	15.94 $\pm$ 1.74*

NOTE. Indirect calorimetry data for 8-week-old NZO/HILt males fed control diet or CL-supplemented diet starting at 6 weeks of age. Respiratory exchange ratio (RER) and energy expenditure (EE) were measured for a 3-day period as described in the methods. Data are expressed as mean  $\pm$  SD for daily (24 hour), dark (12 hour), or light (12 hour) cycle periods for 4 control and 5 CL316,243-fed mice.

Differences were significant by 2-way ANOVA at \* $P < .005$ , † $P < .01$ , and ‡ $P < .05$ . There were no significant differences in automated measures of total activity (data not shown).

to elucidate the metabolic and molecular events driving obesity-induced diabetes (diabesity). Hence, early-manifesting defects in energy homeostasis in untreated NZO/HILt males drive many of the diabesity-associated endocrine changes that occur during later maturational stages. Although CL failed to suppress hyperphagia, and indeed exacerbated it, this compound nonetheless significantly ameliorated defects in energy metabolism to stimulate more normal growth parameters and thus circumvents the severe early-onset obesity required to drive diabesity development in this model. The drug effects that produced a more normal pattern of energy metabolism were not associated with any change in physical activity. Since NZO mice reportedly exhibit a defect in leptin transport rather than in either the receptor or its ligand,<sup>9</sup> the exacerbated food consumption mediated by CL may be a reflection of its ability to suppress the progressive increase in serum leptin concentration observed in controls, and thus reduce transport across the blood-brain barrier even more than in controls.

The loss of weight was determined to be primarily associated with loss of adiposity in the CL-fed NZO mice as indicated by the decreased fat pad weights of 8- and 22-week-old NZO/HILt mice at the time of necropsy (Table 2). Another important observation was that the white fat tissue, especially the inguinal and retroperitoneal depots, of the CL-fed mice was darker and brown in color and appeared to be taking on the characteristics of BAT. Histology (Fig 3E and F) and gene expression analysis (Table 3 and Fig 4) verified increased accumulation of brown adipocytes and UCP-1 mRNA expression in the white adipose tissue depots in 2 independent cohorts of animals fed dietary CL for 4 and 18 weeks. Similar multilocular adipocytes, shown to be positive for UCP-1 by immunohistochemistry, have been observed in inguinal fat and retroperitoneal fat of mice after  $\beta_3$ -adrenergic stimulation using CL and cold exposure.<sup>27</sup> These results are intriguing since it had previously been shown that

CL's effects on the induction of brown adipocytes in traditional white adipose tissue depots vary considerably between inbred mouse strains and is highly correlated with weight loss by  $\beta_3$ -adrenergic stimulation.<sup>17,27</sup> Collins et al<sup>17</sup> had demonstrated that CL prevented diet-induced obesity from occurring in A/J mice but failed to prevent diet-induced obesity in C57BL/6J mice, a strain having a diminished response to  $\beta_3$ -adrenergic stimulation. Experiments using diazoxide, a K-adenosine triphosphate (ATP) channel agonist known to suppress hyperinsulinemia, has been shown to restore  $\beta_3$ -adrenergic receptor expression and the efficacy of CL in decreasing adiposity in diet-induced obese C57BL/6J mice.<sup>28</sup> NZO mice have significantly elevated  $\beta_3$ -adrenergic receptor expression (6- to 7-fold; data not shown) in both retroperitoneal and inguinal fat, but no change in BAT after 22 weeks of dietary CL. Although it is not known whether efficacy of CL treatment is diminished in aged hyperinsulinemic NZO mice as observed with obese hyperinsulinemic C57BL/6J animals, it does appear that NZO mice, like A/J, are not refractory to the effects of chronic CL exposure as are C57BL/6J.<sup>17</sup> Furthermore, CL-mediated weight loss in recombinant inbred strains derived from A/J and C57BL/6J mice was strongly associated with the capacity of each strain to induce brown adipocytes in traditional white adipose tissue depots<sup>27</sup> and at least 4 quantitative trait loci have been now linked to this phenotype.<sup>16</sup> NZO mice, like A/J mice, are apparently genetically predisposed to respond to  $\beta_3$ -adrenergic stimulation with increased brown adipocytes in white adipose tissue. PPAR $\alpha$  and PGC-1, transcription factors that regulate genes involved in fatty acid oxidation and mitochondrial biogenesis, respectively, were also more highly expressed in inguinal and retroperitoneal white adipose tissue of CL-fed NZO mice as compared to NZO control animals (Fig 4). Our observations suggest that the inguinal and retroperitoneal fat depots have at least partially converted into thermogenically active

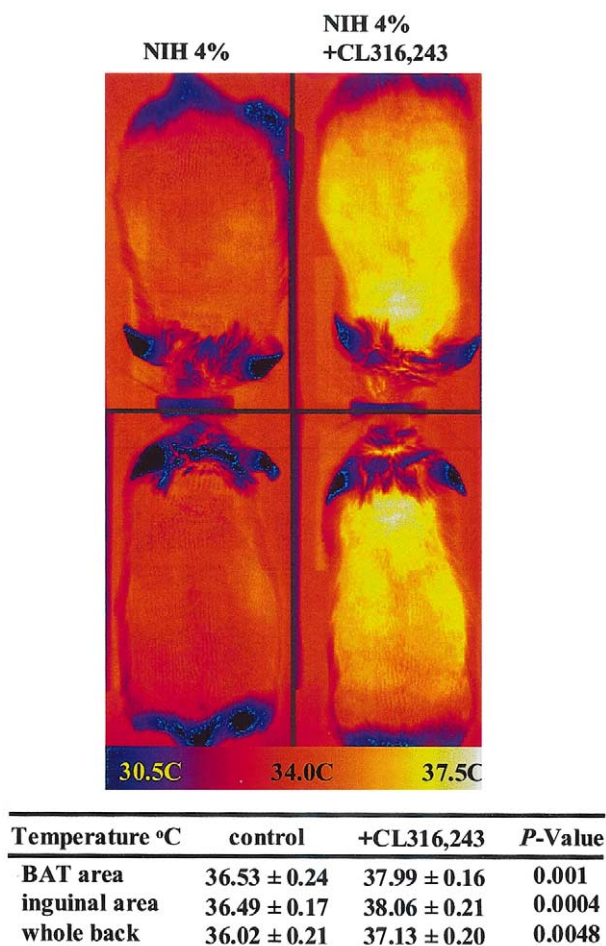


**Fig 5.** CL316,243-mediated increases in whole body thermogenesis measured by thermal signature analysis. This image represents the dramatic increase of body temperature by CL (right panels) compared to control mice (left panels). Thermographic imaging on all 4 mice was performed simultaneously. Dorsal, scapular and inguinal temperature were measured as described in the methods. Data in the table represents the mean  $\pm$  SEM for 8-week-old NZO/HILt males fed control or CL-supplemented diet starting at 4 weeks of age ( $n = 8$  per group).

BAT capable of utilizing fatty acids for production of heat via uncoupling of oxidative phosphorylation. These changes would create a negative energy balance and subsequent loss of fat content within these tissues.

Thermal signature analysis of CL-fed NZO mice measured substantial temperature increases on areas of the back directly adjacent to the inguinal and interscapular BAT depots (Fig 5). The magnitude of this temperature difference, approximately 1.5°C, demonstrates significantly increased oxidative metabolism via brown fat thermogenesis. Several reports using rodent models of obesity have also demonstrated weight loss associated with increased brown adipocyte thermogenesis following CL treatment.<sup>14,21,22,27,29</sup> Although the caloric output caused by chronically increased thermogenesis is difficult to determine, it is clearly sufficient to prevent weight gain and adiposity in spite of increased caloric intake by these animals. Increased amino

acid catabolism in CL-fed mice may provide an alternative mechanism to generate energy required to maintain increased caloric output via thermogenesis.

Indirect calorimetry experiments confirmed our observations of increased energy expenditure by NZO mice fed CL, and also showed a marked improvement in control of nutrient partitioning in the switch from the light to the dark cycle. Our data show both significantly increased heat generation and RER, especially during the night following only 2 weeks of CL-feeding. Since postprandial fat oxidation is inhibited, even when the fat content of the diet is substantial,<sup>30-32</sup> the increased nighttime RER of CL-fed mice (eg, switch from fat to carbohydrate metabolism) could reflect greater carbohydrate intake due to increased hyperphagia. If so, the low fat content (4%) of the diet used in our study may accentuate the large CL-mediated increases in RER.

A survey of almost 30 genes in 8-week-old NZO mice fed NIH 4%  $\pm$  CL showed significant differences of expression in adipsin, which was decreased 14-fold in liver and increased almost 11-fold in muscle. Adipsin, or complement D, a subunit of the ASP complex, is important for triglyceride synthesis and lipid clearance.<sup>33,34</sup> Since liver histopathology of CL-fed mice showed significantly less fat accumulation than controls (Fig 3C and D), it may be likely that decreased triglyceride synthesis via reduced ASP complex function leads to decreased hepatic lipidosis. Several reports using mouse models have demonstrated a relationship between adipsin mRNA expression and hepatic steatosis.<sup>35,36</sup> It is also important to note that significantly decreased hepatic adipsin (14-fold) in CL-treated mice may have resulted in plasma triglyceride levels that are 5-fold lower compared to control animals. Since adipsin is presumably expressed only in adipocytes and hepatocytes, the increase of adipsin in muscle is not clearly understood. HSL, induced by CL treatment in both muscle and inguinal fat, but unchanged in liver, may be the result of increased tissue demand for fatty acids required as fuel for  $\beta_3$  adrenergically-induced thermogenic mechanisms. The expression of UCP-3 in muscle was also decreased approximately 4.5-fold in CL-fed NZO/HILt mice. Since UCP-3 can be regulated in muscle by leptin and free fatty acids,<sup>37,38</sup> its decreased expression could be explained by the efficacy of CL treatment in lowering plasma leptin levels in the NZO/HILt mice. Several laboratories have published contradictory reports regarding the effect of acute or chronic CL treatment on muscle UCP-3 expression.<sup>37,39,40</sup> Direct effects of CL on muscle are not likely due of lack of  $\beta_3$ -adrenergic receptors in this tissue. Human studies have demonstrated a strong relationship between the expression of genes coregulated by oxidative phosphorylation (OXPHOS-CR) in skeletal muscle with both aerobic capacity ( $VO_{2max}$ ) and T2D.<sup>41,42</sup> Increasing PGC-1 $\alpha$  expression in skeletal muscle of mice by an adenoviral expression vector was able to upregulate OXPHOS-CR genes, suggesting a role for PGC-1 $\alpha$  in OXPHOS-CR gene regulation and diabetes.<sup>43</sup> Our analysis of 8-week-old NZO mice fed chow or chow supplemented with CL showed very little variation of skeletal muscle PGC-1 $\alpha$  (data not shown), suggesting that increased energy expenditure in the CL-animals is not a result of elevated oxidative capacity in muscle.

Although the mechanism by which chronic CL exposure



prevents diabetes in NZO/HILt males is not completely understood, the results we present suggest that altered partitioning of energy associated with increased energy expenditure by brown fat thermogenesis may play a significant role. Since  $\beta_3$ -adrenergic receptors are predominantly expressed in white and brown adipose tissue, these tissues play an integral role in the antidiabetes mechanism of  $\beta_3$  adrenergic stimulation. Experiments using a mouse model with a targeted deletion for the  $\beta_3$ -adrenergic receptor in which tissue-specific  $\beta_3$ -receptor transgenes are reintroduced into white and brown fat, or brown fat alone, demonstrated that the efficacy of CL requires  $\beta_3$

adrenergic stimulation of white, but not brown fat.<sup>44</sup> Overall, these data indicate that  $\beta_3$ -adrenergic receptor activation may circumvent some of the metabolic defects caused by peripheral leptin resistance and/or impaired sympathetic afferents in NZO mice.

#### ACKNOWLEDGMENT

Dr Anthony Nicolson and Crystal Davis are thanked for assistance in operation of the automated metabolic caging systems. The authors gratefully acknowledge the expert technical assistance of Jenn Kintner, Bruce Regimbal, and Pamela Stanley.

#### REFERENCES

1. Elbein SC: Perspective: The search for genes for type 2 diabetes in the post-genome era. *Endocrinology* 143:2012-2018, 2002
2. Bouchard C: Genetics and the metabolic syndrome. *Int J Obes Relat Metab Disord* 19:S52-59, 1995 (suppl 1)
3. Reifsnyder PC, Leiter EH: Deconstructing and reconstructing obesity-induced diabetes (diabetes) in mice. *Diabetes* 51:825-832, 2002
4. Reifsnyder PC, Churchill G, Leiter EH: Maternal environment and genotype interact to establish diabetes in mice. *Genome Res* 10:1568-1578, 2000
5. Plum L, Giesen K, Kluge R, et al: Characterisation of the mouse diabetes susceptibility locus Nidd/SJL: Islet cell destruction, interaction with the obesity QTL Nob1, and effect of dietary fat. *Diabetologia* 45:823-830, 2002
6. Taylor BA, Wnek C, Schroeder D, et al: Multiple obesity QTLs identified in an intercross between the NZO (New Zealand Obese) and the SM (small) mouse strains. *Mamm Genome* 12:95-103, 2001
7. Igel M, Becker W, Herberg L, et al: Hyperleptinemia, leptin resistance, and polymorphic leptin receptor in the New Zealand obese mouse. *Endocrinology* 138:4234-4239, 1997
8. Halaas JL, Boozer C, Denton DA, et al: Physiological response to long-term peripheral and central leptin infusion in lean and obese mice. *Proc Natl Acad Sci USA* 94:8878-8883, 1997
9. Hileman SM, Pierroz DD, Masuzaki H, et al: Characterization of short isoforms of the leptin receptor in rat cerebral microvessels and of brain uptake of leptin in mouse models of obesity. *Endocrinology* 143:775-783, 2002
10. Veroni M, Proietto J, Larkins R: Evolution of insulin resistance in New Zealand Obese mice. *Diabetes* 40:1480-1487, 1991
11. Andrikopoulos S, Rosella G, Kaczmarczyk SJ, et al: Impaired regulation of hepatic fructose-1,6-bisphosphatase in the New Zealand Obese mouse: An acquired defect. *Metabolism* 45:622-626, 1996
12. Flurkey K, Rosen C, Partke H-J, et al: Rapid maturational growth as a predictor of NIDDM in NZO male mice. *Diabetes* 47:A318, 1998 (suppl 1, abstr)
13. Collins S, Daniel KW, Rohlf EM: Depressed expression of adipocyte beta-adrenergic receptors is a common feature of congenital and diet-induced obesity in rodents. *Int J Obes Relat Metab Disord* 23:669-677, 1999
14. Himms-Hagen J, Cui J, Danforth E Jr, et al: Effect of CL-316,243, a thermogenic beta 3-agonist, on energy balance and brown and white adipose tissues in rats. *Am J Physiol* 266:R1371-1382, 1994
15. Watkins SM, Reifsnyder PC, Pan H-J, et al: Lipid metabolome-wide effects of the peroxisome proliferator-activated receptor gamma agonist rosiglitazone on a new mouse model of type 2 diabetes. *J Lipid Res* 43:1809-1817, 2002
16. Koza RA, Hohmann SM, Guerra C, et al: Synergistic gene interactions control the induction of the mitochondrial uncoupling protein (Ucp1) gene in white fat tissue. *J Biol Chem* 275:34486-34492, 2000
17. Collins S, Daniel KW, Petro AE, et al: Strain-specific response (suppl) to beta 3-adrenergic receptor agonist treatment of diet-induced obesity in mice. *Endocrinology* 138:405-413, 1997
18. Ridgway ND, Vance DE: Purification of phosphatidylethanolamine N-methyltransferase from rat liver. *J Biol Chem* 262:17231-17239, 1987
19. Kodaki T, Yamashita S: Yeast phosphatidylethanolamine methylation pathway. Cloning and characterization of two distinct methyltransferase genes. *J Biol Chem* 262:15428-15435, 1987
20. Cui Z, Vance JE, Chen MH, et al: Cloning and expression of a novel phosphatidylethanolamine N-methyltransferase. A specific biochemical and cytological marker for a unique membrane fraction in rat liver. *J Biol Chem* 268:16655-16663, 1993
21. Yoshida T, Sakane N, Wakabayashi Y, et al: Anti-obesity and anti-diabetic effects of CL 316,243, a highly specific beta 3-adrenoceptor agonist, in yellow KK mice. *Life Sci* 54:491-498, 1994
22. Umekawa T, Yoshida T, Sakane N, et al: Anti-obesity and anti-diabetic effects of CL316,243, a highly specific beta 3-adrenoceptor agonist, in Otsuka Long-Evans Tokushima Fatty rats: Induction of uncoupling protein and activation of glucose transporter 4 in white fat. *Eur J Endocrinol* 136:429-437, 1997
23. Liu X, Perusse F, Bukowiecki LJ: Mechanisms of the antidiabetic effects of the beta 3-adrenergic agonist CL-316243 in obese Zucker-ZDF rats. *Am J Physiol* 274:R1212-1219, 1998
24. Tsujii S, Bray GA: A beta-3 adrenergic agonist (BRL-37,344) decreases food intake. *Physiol Behav* 63:723-728, 1998
25. Haskell BD, Flurkey K, Duffy TM, et al: The diabetes-prone NZO/HILt Strain. I. Immunophenotypic comparison to the related NZB/BinJ and NZW/LacJ strains. *Lab Invest* 82:833-842, 2002
26. Junger E, Herberg L, Jeruschke K, et al: The diabetes-prone NZO/HI strain: II. Pancreatic immunopathology. *Lab Invest* 82:843-853, 2002
27. Guerra C, Koza RA, Yamashita H, et al: Emergence of brown adipocytes in white fat in mice is under genetic control. Effects on body weight and adiposity. *J Clin Invest* 102:412-420, 1998
28. Surwit RS, Dixon TM, Petro AE, et al: Diazoxide restores b3-adrenergic receptor function in diet-induced obesity and diabetes. *Endocrinology* 141:3630-3637, 2000
29. Yoshida T, Sakane N, Wakabayashi Y, et al: Anti-obesity effect of CL 316,243, a highly specific beta 3-adrenoceptor agonist, in mice with monosodium-L-glutamate-induced obesity. *Eur J Endocrinol* 131:97-102, 1994
30. Griffiths AJ, Humphreys SM, Clark ML, et al: Immediate metabolic availability of dietary fat in combination with carbohydrate. *Am J Clin Nutr* 59:53-59, 1994
31. Flatt JP, Ravussin E, Acheson KJ, et al: Effects of dietary fat on postprandial substrate oxidation and on carbohydrate and fat balances. *J Clin Invest* 76:1019-1024, 1985
32. Flatt JP: Body composition, respiratory quotient, and weight maintenance. *Am J Clin Nutr* 62:1107S-1117S, 1995 (suppl)

33. Cianflone K: Acylation stimulating protein and the adipocyte. *J Endocrinol* 155:203-206, 1997
34. Cianflone K, Xia Z, Chen LY: Critical review of acylation-stimulating protein physiology in humans and rodents. *Biochim Biophys Acta* 1609:127-143, 2003
35. Yu S, Matsusue K, Kashireddy P, et al: Adipocyte-specific gene expression and adipogenic steatosis in the mouse liver due to peroxisome proliferator-activated receptor gamma1 (PPARgamma1) overexpression. *J Biol Chem* 278:498-505, 2003
36. Gregoire FM, Zhang Q, Smith SJ, et al: Diet-induced obesity and hepatic gene expression alterations in C57BL/6J and ICAM-1-deficient mice. *Am J Physiol Endocrinol Metab* 282:E703-713, 2002
37. Gong DW, He Y, Karas M, et al: Uncoupling protein-3 is a mediator of thermogenesis regulated by thyroid hormone, beta3-adrenergic agonists, and leptin. *J Biol Chem* 272:24129-24132, 1997
38. Weigle DS, Selfridge LE, Schwartz MW, et al: Elevated free fatty acids induce uncoupling protein 3 expression in muscle: A potential explanation for the effect of fasting. *Diabetes* 47:298-302, 1998
39. Nakamura Y, Nagase I, Asano A, et al: Beta 3-adrenergic agonist up-regulates uncoupling proteins 2 and 3 in skeletal muscle of the mouse. *J Vet Med Sci* 63:309-314, 2001
40. Yoshitomi H, Yamazaki K, Abe S, et al: Differential regulation of mouse uncoupling proteins among brown adipose tissue, white adipose tissue, and skeletal muscle in chronic beta 3 adrenergic receptor agonist treatment. *Biochem Biophys Res Commun* 253:85-91, 1998
41. Eriksson KF, Lindgarde F: Impaired glucose tolerance in a middle-aged male urban population. *Diabetologia* 45:526-531, 1990
42. Mootha VK, Lindgren CM, Eriksson K-F, et al: PGC-1 $\alpha$ -responsive genes involved in oxidative phosphorylation are coordinately downregulated in human diabetes. *Nat Genet* 34:267-273, 2003
43. Lin J, Wu H, Tarr PT, et al: Transcriptional co-activator PGC-1 $\alpha$  drives the formation of slow-twitch muscles fibres. *Nature* 418:797-801, 2002
44. Grujic D, Susulic VS, Harper ME, et al: Beta3-adrenergic receptors on white and brown adipocytes mediate beta3-selective agonist-induced effects on energy expenditure, insulin secretion, and food intake. A study using transgenic and gene knockout mice. *J Biol Chem* 272:17686-17693, 1997